

**ERINDA**   
European Research Infrastructures  
for Nuclear Data Applications

# ERINDA

## workshop

*organized by the CERN EN-STI group on behalf of the n\_TOF Collaboration*

CERN, Geneva, Switzerland - 1-3 October 2013

# PROCEEDINGS

**CERN-Proceedings-2014-002**

**ISBN 978-92-9083-403-8**

Copyright © The Authors, 2014.

Published by CERN.

Selection and/or peer-review under responsibility of the Organizing Committee for the ERINDA Workshop.

**This volume should be cited as:**

Proceedings of the ERINDA Workshop, CERN, Geneva, Switzerland, 1-3 October 2013, edited by Enrico Chiaveri, CERN-Proceedings-2014-002 (CERN, Geneva, 2014).

**A contribution in this volume should be cited as:**

[Author name(s)], in Proceedings of the ERINDA Workshop, CERN, Geneva, Switzerland, 1-3 October 2013, edited by Enrico Chiaveri, CERN-Proceedings-2014-002 (CERN, Geneva, 2014), pp. [first page] - [last page].

# Measurement of the $^{240,242}\text{Pu}(n,f)$ cross section at the CERN n\_TOF facility

A. Tsinganis<sup>1,2</sup>, E. Berthoumieux<sup>3</sup>, C. Guerrero<sup>2</sup>, N. Colonna<sup>4</sup>, M. Calviani<sup>2</sup>, R. Vlastou<sup>1</sup>, S. Andriamonje<sup>2</sup>, V. Vlachoudis<sup>2</sup>, F. Gunsing<sup>3</sup>, C. Massimi<sup>5</sup>, S. Altstadt<sup>6</sup>, J. Andrzejewski<sup>7</sup>, L. Audouin<sup>8</sup>, M. Barbagallo<sup>4</sup>, V. Bécaries<sup>9</sup>, F. Bečvář<sup>10</sup>, F. Belloni<sup>3</sup>, J. Billowes<sup>11</sup>, V. Boccone<sup>2</sup>, D. Bosnar<sup>12</sup>, M. Brugger<sup>2</sup>, F. Calviño<sup>13</sup>, D. Cano-Ott<sup>9</sup>, C. Carrapiço<sup>14</sup>, F. Cerutti<sup>2</sup>, M. Chin<sup>2</sup>, G. Cortés<sup>13</sup>, M.A. Cortés-Giraldo<sup>15</sup>, M. Diakaki<sup>1</sup>, C. Domingo-Pardo<sup>16</sup>, I. Duran<sup>17</sup>, R. Dressler<sup>18</sup>, N. Dzyysiuk<sup>19</sup>, C. Eleftheriadis<sup>20</sup>, A. Ferrari<sup>2</sup>, K. Fraval<sup>3</sup>, S. Ganesan<sup>21</sup>, A.R. García<sup>9</sup>, G. Giubrone<sup>16</sup>, M.B. Gómez-Hornillos<sup>13</sup>, I.F. Gonçalves<sup>14</sup>, E. González-Romero<sup>9</sup>, E. Griesmayer<sup>22</sup>, P. Gurusamy<sup>20</sup>, A. Hernández-Prieto<sup>2,13</sup>, D.G. Jenkins<sup>23</sup>, E. Jericha<sup>22</sup>, Y. Kadi<sup>2</sup>, F. Käppeler<sup>24</sup>, D. Karadimos<sup>1</sup>, N. Kivel<sup>18</sup>, P. Koehler<sup>25</sup>, M. Kokkoris<sup>1</sup>, M. Krtička<sup>26</sup>, J. Kroll<sup>26</sup>, C. Lampoudis<sup>3</sup>, C. Langer<sup>6</sup>, E. Leal-Cidoncha<sup>16</sup>, C. Lederer<sup>6,27</sup>, H. Leeb<sup>22</sup>, L.S. Leong<sup>8</sup>, R. Losito<sup>2</sup>, A. Mallick<sup>21</sup>, A. Manousos<sup>20</sup>, J. Marganiec<sup>7</sup>, T. Martínez<sup>9</sup>, P.F. Mastinu<sup>19</sup>, M. Mastroianni<sup>4</sup>, M. Meaze<sup>4</sup>, E. Mendoza<sup>9</sup>, A. Mengoni<sup>28</sup>, P.M. Milazzo<sup>29</sup>, F. Mingrone<sup>5</sup>, M. Mirea<sup>30</sup>, W. Mondelaers<sup>31</sup>, C. Paradela<sup>17</sup>, A. Pavlik<sup>27</sup>, J. Perkowski<sup>7</sup>, A. Plompen<sup>31</sup>, J. Praena<sup>14</sup>, J.M. Quesada<sup>14</sup>, T. Rauscher<sup>32</sup>, R. Reifarth<sup>6</sup>, A. Riego<sup>13</sup>, M.S. Robles<sup>17</sup>, F. Roman<sup>2,30</sup>, C. Rubbia<sup>2,33</sup>, M. Sabaté-Gilarte<sup>14</sup>, R. Sarmiento<sup>14</sup>, A. Saxena<sup>21</sup>, P. Schillebeeckx<sup>31</sup>, S. Schmidt<sup>6</sup>, D. Schumann<sup>18</sup>, G. Tagliente<sup>4</sup>, J.L. Tain<sup>16</sup>, D. Tarrío<sup>17</sup>, L. Tassan-Got<sup>8</sup>, S. Valenta<sup>26</sup>, G. Vannini<sup>5</sup>, V. Variale<sup>4</sup>, P. Vaz<sup>14</sup>, A. Ventura<sup>28</sup>, R. Versaci<sup>2</sup>, M.J. Vermeulen<sup>23</sup>, A. Wallner<sup>27</sup>, T. Ware<sup>11</sup>, M. Weigand<sup>6</sup>, C. Weiss<sup>22</sup>, T. Wright<sup>11</sup>, and P. Žugec<sup>12</sup>

<sup>1</sup>National Technical University of Athens (NTUA), Greece

<sup>2</sup>European Organisation for Nuclear Research (CERN), Geneva, Switzerland

<sup>3</sup>Commissariat à l'Énergie Atomique (CEA) Saclay - Irfu, Gif-sur-Yvette, France

<sup>4</sup>Istituto Nazionale di Fisica Nucleare, Bari, Italy

<sup>5</sup>Dipartimento di Fisica e Astronomia, Università di Bologna, and Sezione INFN di Bologna, Italy

<sup>6</sup>Johann-Wolfgang-Goethe Universität, Frankfurt, Germany

<sup>7</sup>Uniwersytet Łódzki, Lodz, Poland

<sup>8</sup>Centre National de la Recherche Scientifique/IN2P3 - IPN, Orsay, France

<sup>9</sup>Centro de Investigaciones Energeticas Medioambientales y Tecnológicas (CIEMAT), Madrid, Spain

<sup>10</sup>Charles University, Prague, Czech Republic

<sup>11</sup>University of Manchester, Oxford Road, Manchester, UK

<sup>12</sup>Department of Physics, Faculty of Science, University of Zagreb, Croatia

<sup>13</sup>Universitat Politècnica de Catalunya, Barcelona, Spain

<sup>14</sup>Instituto Tecnológico e Nuclear, Instituto Superior Técnico, Universidade Técnica de Lisboa, Portugal

<sup>15</sup>Universidad de Sevilla, Spain

<sup>16</sup>Instituto de Física Corpuscular, CSIC-Universidad de Valencia, Spain

<sup>17</sup>Universidade de Santiago de Compostela, Spain

<sup>18</sup>Paul Scherrer Institut, Villigen PSI, Switzerland

<sup>19</sup>Istituto Nazionale di Fisica Nucleare, Laboratori Nazionali di Legnaro, Italy

<sup>20</sup>Aristotle University of Thessaloniki, Thessaloniki, Greece

<sup>21</sup>Bhabha Atomic Research Centre (BARC), Mumbai, India

<sup>22</sup>Atominstytut, Technische Universität Wien, Austria

<sup>23</sup>University of York, Heslington, York, UK

<sup>24</sup>Karlsruhe Institute of Technology, Campus Nord, Institut für Kernphysik, Karlsruhe, Germany

<sup>25</sup>Department of Physics, University of Oslo, Norway

<sup>26</sup>Charles University, Prague, Czech Republic

<sup>27</sup>University of Vienna, Faculty of Physics, Austria

<sup>28</sup>Agenzia nazionale per le nuove tecnologie, l'energia e lo sviluppo economico sostenibile (ENEA), Bologna, Italy

<sup>29</sup>Istituto Nazionale di Fisica Nucleare, Trieste, Italy

<sup>30</sup>Horia Hulubei National Institute of Physics and Nuclear Engineering - IFIN HH, Bucharest - Magurele, Romania

<sup>31</sup>European Commission JRC, Institute for Reference Materials and Measurements, Geel, Belgium

<sup>32</sup>Department of Physics and Astronomy - University of Basel, Basel, Switzerland

<sup>33</sup>Laboratori Nazionali del Gran Sasso dell'INFN, Assergi (AQ), Italy

## Abstract

Knowledge of neutron cross sections of various plutonium isotopes and other minor actinides is crucial for the design of advanced nuclear systems. The  $^{240,242}\text{Pu}(n,f)$  cross sections were measured at the CERN n\_TOF facility, taking advantage of the wide energy range (from thermal to GeV) and the high instantaneous flux of the neutron beam. In this work, preliminary results for  $^{242}\text{Pu}$  are presented along with a theoretical cross section calculation performed with the EMPIRE code.

## 1 Introduction

The sustainable use of nuclear energy as a means of reducing reliance on fossil-fuel for energy production has motivated the development of nuclear systems characterised by a more efficient use of nuclear fuels, a lower production of nuclear waste, economic viability and competitiveness and minimal risk of proliferation of nuclear material and is being pursued by international collaborations [1,2]. The accurate knowledge of relevant nuclear data, including neutron cross sections of a variety of plutonium isotopes and other minor actinides, is crucial for feasibility and performance studies of advanced nuclear systems.

In particular, the  $^{240}\text{Pu}$  and  $^{242}\text{Pu}$  isotopes are produced in thermal and fast reactors by successive neutron captures and  $\beta$ - or  $\alpha$ - decays. Both isotopes are non-fissile and therefore unsuitable for recycling in a thermal reactor, due to their low fission cross-section. Furthermore, they are typically produced faster than they are transmuted due to their relatively long half-life. A more efficient burning via fission would occur with the harder neutron spectrum of a fast reactor.

In this context, the  $^{240,242}\text{Pu}(n,f)$  cross sections were measured at n\_TOF relative to the well-known  $^{235}\text{U}(n,f)$  cross section. These isotopes are included in the Nuclear Energy Agency (NEA) High Priority List [3] and the NEA WPEC Subgroup 26 Report on the accuracy of nuclear data for advanced reactor design [4].

The high  $\alpha$ -activity ( $\sim 6.5$  MBq/sample) of the  $^{240}\text{Pu}$  samples significantly complicates the analysis of the obtained data. The very high  $\alpha$ -pile-up probability affects the pulse-height spectrum and significantly reduces the quality of the separation of  $\alpha$ -particles and fission fragments. Furthermore, a significant deterioration of the detector performance was observed in the detectors exposed to the  $^{240}\text{Pu}$  samples. For the above reasons, only preliminary results for the  $^{242}\text{Pu}(n,f)$  measurement are presented in this work.

## 2 Experimental setup

### 2.1 The n\_TOF facility

The experiment was carried out at the CERN n\_TOF facility [5–7]. At n\_TOF, neutrons are produced through spallation induced by a 20 GeV/c bunched proton beam impinging on a massive lead target and subsequent moderation in a few centimetres thick layer of (borated) water. The produced neutrons have energies starting from thermal and up to over 10 GeV and travel along an approximately 185 m long path to reach the experimental area. This allows to cover a very extended energy region in a single experiment, thus reducing uncertainties related to different measurements performed in separate neutron

energy ranges. The high instantaneous flux of the n\_TOF neutron beam mitigates the adverse effects of the strong  $\alpha$ -particle background produced by the samples and the low fission cross section below and near the fission threshold.

## 2.2 Samples

Eight plutonium oxide ( $\text{PuO}_2$ ) samples manufactured at IRMM, Geel, were used [8] ( $4 \times {}^{240}\text{PuO}_2$ ,  $4 \times {}^{242}\text{PuO}_2$ ), for a total mass of 3.1 mg of  ${}^{240}\text{Pu}$  ( $\sim 0.11 \text{ mg/cm}^2$  per sample, 99.90% purity) and 3.6 mg of  ${}^{242}\text{Pu}$  ( $\sim 0.13 \text{ mg/cm}^2$  per sample, 99.97% purity). The material was electro-deposited on an aluminium backing 0.25 mm thick and 5 cm in diameter, while the deposit itself had a diameter of 3 cm. Various contaminants were present, mainly in the form of other plutonium isotopes, such as  ${}^{238}\text{Pu}$ ,  ${}^{239}\text{Pu}$ ,  ${}^{241}\text{Pu}$  and  ${}^{244}\text{Pu}$ . While these impurities are present in very small amounts, the high fission cross sections of fissionable contaminants compared to the isotopes of interest dominate in parts of the energy range studied.

Additionally, a  ${}^{235}\text{U}$  sample ( $\text{UF}_4$ ) with a mass of 18 mg deposited on a 0.2 mm thick aluminium backing was used as reference. Since this sample had a diameter of 7 cm, its active area was reduced with a thin aluminium mask to match the diameter of the plutonium samples. The active mass was therefore reduced to 3.3 mg of  ${}^{235}\text{U}$  ( $\sim 0.47 \text{ mg/cm}^2$ ).

## 2.3 Detectors and data acquisition

The measurements were performed with Micromegas (Micro-MESH Gaseous Structure) gas detectors [9, 10]. The gas volume of the Micromegas is separated into a charge collection region (several mm) and an amplification region (typically tens of  $\mu\text{m}$ ) by a thin “micromesh” with 35  $\mu\text{m}$  diameter holes on its surface. The amplification that takes place in the amplification region significantly improves the signal-to-noise ratio of the detector. This is of special importance for the high neutron energy region, where the fission signals are recorded within a few  $\mu\text{s}$  of the  $\gamma$ -flash (see section 3.2). A chamber capable of holding up to 10 sample-detector modules was constructed and used to house the plutonium and uranium samples. The chamber was filled with an  $\text{Ar}:\text{CF}_4:\text{isoC}_4\text{H}_{10}$  gas mixture (88:10:2) at a pressure of 1 bar and under constant circulation.

Existing electronics from previous fission measurements were used for signal shaping. Additional electronic protection was added to the pre-amplifier channels to prevent breakage, while the mesh voltage value was chosen to minimize the number of sparks and subsequent trips. Furthermore, the shielding of the pre-amplifier module was improved to mitigate the baseline oscillation observed following the prompt  $\gamma$ -flash. The standard n\_TOF Data Acquisition System [5] based on 8-bit Acqiris flash-ADCs was used for recording and storing the raw data collected by the detectors at a sampling rate of 100 MHz.

Due to the low expected count rate for the measurement, the chamber was placed in the n\_TOF experimental area for several months and in parallel with other measurements performed at n\_TOF. Throughout the measurement, beam-off data were acquired in order to record the  $\alpha$ - and spontaneous fission background produced by the samples.

## 2.4 Experimental issues

The analysis of the experimental data is complicated by certain features of the experimental setup and by sample-induced backgrounds. These include the baseline oscillation induced by the prompt “ $\gamma$ -flash” which is discussed in section 3.2 and the spontaneous fission background, particularly in the case of  ${}^{242}\text{Pu}$ .

While the above factors can be dealt with, an unexpected effect of the high  $\alpha$ -activity of the samples ( $>6 \text{ MBq}$  for  ${}^{240}\text{Pu}$ ) was encountered. After the end of the measurement, a visual inspection of the detectors used with the  ${}^{240}\text{Pu}$  samples revealed a remarkable feature. As seen in fig. 1 (left panel), an obvious circular discolouration of the mesh whose dimension and position exactly matched those of the samples was observed. Upon closer inspection with a microscope (fig. 1, right panel), it became clear

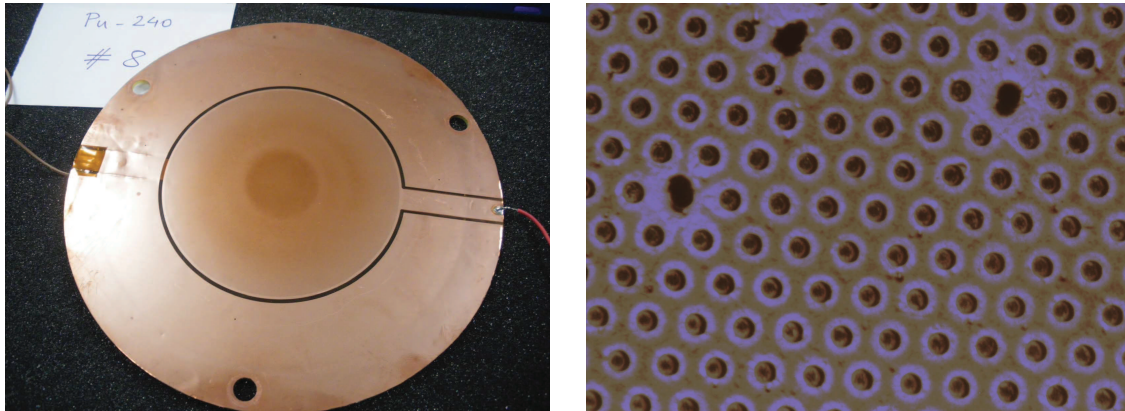


**Fig. 1:** Left: One of the Micromegas detectors used with a  $^{240}\text{Pu}$  sample pictured after the end of the measurement. A 3 cm diameter discolouration is visible on the micromesh. Right: Picture of the micromesh taken with an electronic microscope. Mechanical damage around the rims of the holes can be observed. This leads to a severe deterioration of the detector gain and performance.

that the micromesh had suffered serious mechanical damage, particularly around the rims of the holes which were evidently deformed.

The mechanical damage suffered by the detectors must lead to a deterioration of the electrical field and therefore of the detector gain and overall performance. Indeed, this was clearly observed in the  $^{240}\text{Pu}$  data, where fission fragment and  $\alpha$ -particle signals eventually became virtually indistinguishable in the obtained pulse height spectra. Because of this, a considerable part of the  $^{240}\text{Pu}$  data must be discarded, partially compromising the measurement. Although there was no visible damage, a similar but less pronounced effect was observed in the  $^{242}\text{Pu}$  data, in the form of a slow but non-negligible gain shift throughout the duration of the measurement. The data, therefore, need to be analysed in smaller subsets where the gain can be considered constant.

For the above reasons, preliminary results on  $^{242}\text{Pu}$  only are being presented in this report.

### 3 ANALYSIS AND RESULTS

#### 3.1 Raw data analysis

The raw data from each detector are analysed by means of a pulse recognition routine that determines the amplitude and position in time of the detected signals, among other quantities. The signal baseline is determined by analysing the pre-trigger and post-acquisition window data, accounting for possible signals ( $\alpha$  or spontaneous fission) that may be present. Since the Pu samples are in the same chamber as the  $^{235}\text{U}$  it can be assumed that they receive the same neutron flux, while the fission count rates are sufficiently low to ignore pile-up effects.

#### 3.2 The high neutron energy region

The interactions of the proton beam with the spallation target lead to a significant production of prompt  $\gamma$ -rays and other relativistic particles that travel to the experimental area at (nearly) the speed of light and constitute the bulk of what is commonly termed the “ $\gamma$ -flash”. In Micromegas detectors, this causes an initial signal lasting a few hundred ns, followed by a baseline oscillation that lasts for several  $\mu\text{s}$  or, in terms of neutron energy, down to 1-2 MeV. This behaviour can be observed in fig. 2 (top panel), where the baseline oscillations are clearly visible.

This problem can be mitigated by applying a software “compensation” technique [11] to the digitally recorded data. This method is based on the observation that the oscillations recorded in adjacent

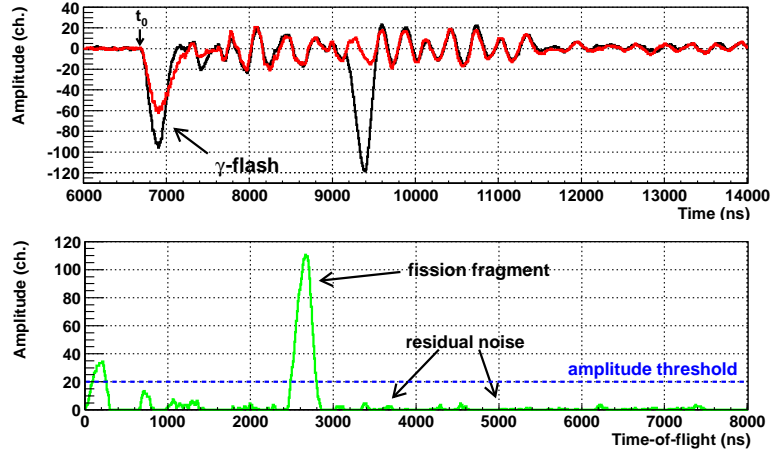


**Fig. 2:** Top panel: The beginning (first few  $\mu\text{s}$ ) of the recorded signals during the same proton bunch from two adjacent detectors. The  $\gamma$ -flash signal and the baseline oscillations are clearly visible. Bottom panel: the residual signal after the subtraction of the two signals above. The oscillation is almost entirely suppressed.

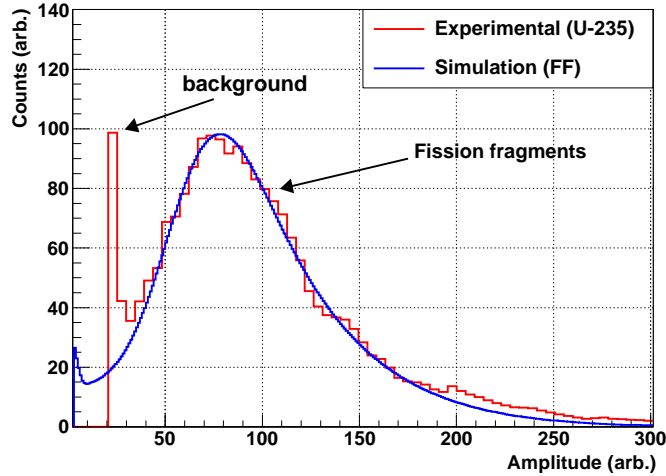


**Fig. 3:** Experimental (red) and simulated (blue) pulse height spectra for  $^{235}\text{U}$ . The cut-off of the low-amplitude signals is due to the threshold set in the peak-search routine.

detectors for the same proton bunch are almost identical. This can be seen by comparing the recorded signals from two detectors placed consecutively in the chamber (fig. 2, top panel). The subtraction of the output of adjacent detectors causes the oscillations to largely cancel each other out, leaving a residual signal that consists primarily of signals attributable either to fission fragments or  $\alpha$ -particles (fig. 2, bottom panel). This signal is then analysed with the peak search routine used for the lower energy region, thus extracting the desired pulse height spectra. The small residual of electronic noise is generally well below the amplitude threshold for fission fragment detection.

### 3.3 Monte-Carlo simulations

The behaviour of the detectors was studied by means of Monte Carlo simulations performed with the FLUKA code [12, 13], focusing particularly on the reproduction of the pulse height spectra of  $\alpha$ -particles and fission fragments for the evaluation of the detector efficiency and the quality of the peak-search routine. In fig. 3, an experimental pulse height spectrum obtained from  $^{235}\text{U}$  and a simulated fission

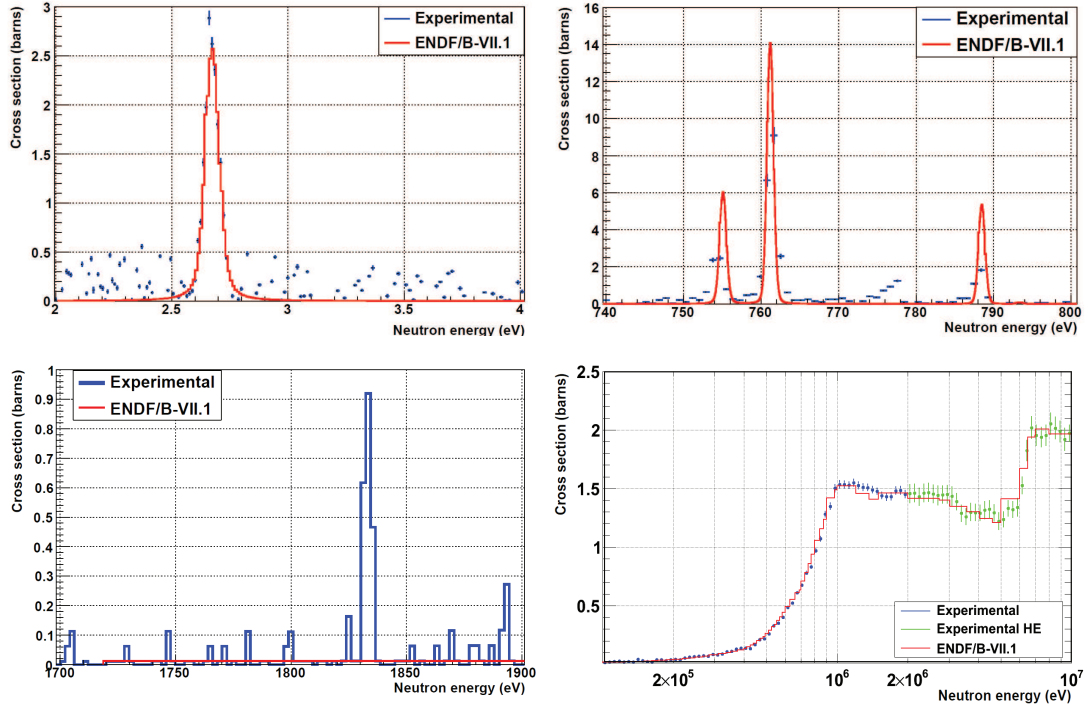


**Fig. 4:** The first  $^{242}\text{Pu}$  resonance at 2.7 eV (top left panel) and resolved resonances between 750 and 800 eV (top right) and around 1800 eV (bottom left). Data above the fission threshold (bottom right). Above 2 MeV, data are treated with the method described in section 3.2. The use of this CPU-intensive method means only a subset of the available statistics has been processed, hence the larger uncertainties pictured here.

fragment spectrum can be compared.

### 3.4 Present results

The spontaneous fission background dominates the low energy region and remains visible up to about 10 keV. Still, several resonances can be observed above this background. The first  $^{242}\text{Pu}$  resonance at  $\sim 2.7$  eV can be seen in the top left panel of Fig. 4, after subtraction of the spontaneous fission background, as determined with a fit of the beam-off data. The top right and bottom left panels show resolved resonances in the 700-800 eV region and up to approximately 1900 eV, including one at  $\sim 780$  eV and one at  $\sim 1830$  eV not present in the evaluated libraries and, at a preliminary analysis, not attributable to any of the stated sample impurities. Additional resonance candidates at higher energies have been observed. Data above 1 keV are shown in the bottom right panel of Fig. 4. The data displayed are combined from the two analysis methods; the conventional “straightforward” analysis, which fails above about 2 MeV due to the baseline oscillations, and the high-energy analysis described in section 3.2. The analysis of the high energy region will be extended up to several tens of MeV.

## 4 THEORETICAL CALCULATIONS

A theoretical calculation of the  $^{242}\text{Pu}(n,f)$  cross section was performed with the EMPIRE nuclear reaction model code [14] (version 3.1). The level densities of the nuclei involved in the calculations were treated within the framework of the Enhanced Generalised Superfluid Model (EGSM). The initial values used

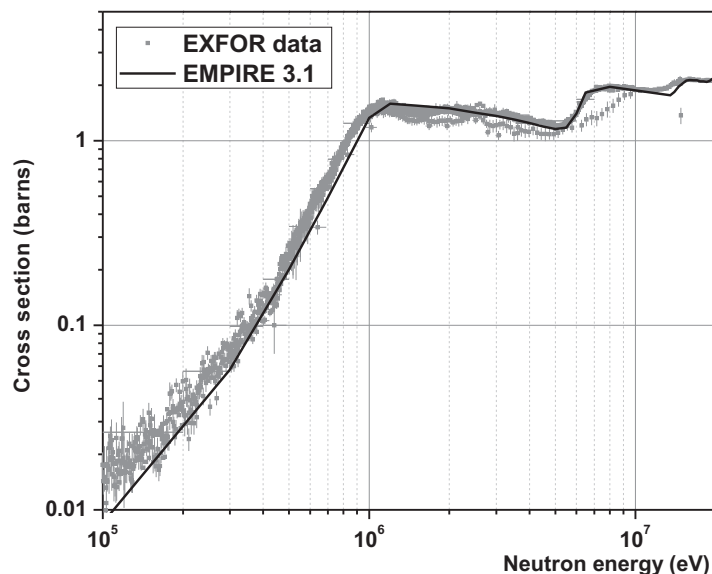


**Fig. 5:** Theoretical calculation of the  $^{242}\text{Pu}(n,f)$  cross section performed with the EMPIRE code, with experimental data retrieved from the EXFOR database.

for the fission barrier parameters (barrier height and width) were retrieved from the RIPL-3 library [15] and subsequently adjusted to better reproduce the experimental data. Preliminary results can be seen in Fig. 5.

## 5 CONCLUSIONS

Preliminary results from the  $^{242}\text{Pu}(n,f)$  experiment performed at the CERN n\_TOF facility are presented. The experimental setup and analysis method is described, including auxiliary Monte-Carlo simulations and an off-line technique to recover high-neutron energy data affected by the prompt  $\gamma$ -fission.

Analysis of the  $^{242}\text{Pu}(n,f)$  data is well under way and is only complicated by the gradual detector gain shift. Among the issues still to be addressed are the exact determination of the detector efficiency and the amplitude threshold correction, the accurate subtraction of the spontaneous fission background and the estimation of all uncertainties involved. The analysis of the high-energy region data is particularly CPU-intensive and is therefore proceeding at a relatively slow pace, given the amount of data acquired during the measurement.

Finally, a significant part of the  $^{240}\text{Pu}(n,f)$  was discarded due to the damage suffered by the detectors, as explained in section 2.4. Even under normal detector operation, the high  $\alpha$ -pileup probability (>30%) produces a long tail in the amplitude spectra that adversely affects the  $\alpha$ -fission fragment separation. In order not to set a very high amplitude threshold that would further reduce the statistics, an alternative approach – characterising and subtracting the  $\alpha$ -background – will be employed.

## References

- [1] Generation-IV International Forum, [www.gen-4.org/](http://www.gen-4.org/)
- [2] International Framework for Nuclear Energy Cooperation (IFNEC), [www.ifnec.org/](http://www.ifnec.org/)
- [3] NEA Nuclear Data High Priority Request List, [www.nea.fr/html/dbdata/hpr1/](http://www.nea.fr/html/dbdata/hpr1/)
- [4] OECD/NEA WPEC Subgroup 26 Final Report, [www.nea.fr/html/science/wpec/volume26/volume26.pdf/](http://www.nea.fr/html/science/wpec/volume26/volume26.pdf/)
- [5] U. Abbondanno, Tech. Rep. CERN-SL-2002-053 ECT, CERN, Geneva (2002)

- [6] C. Guerrero et al., Eur. Phys. J. A **49**, 1 (2013)
- [7] E. Berthoumieux, [cds.cern.ch/record/1514680?ln=en](https://cds.cern.ch/record/1514680?ln=en)
- [8] G. Sibbens et al., J. Radioanal. Nucl. Chem. (2013) [dx.doi.org/10.1007/s10967-013-2668-7](https://doi.org/10.1007/s10967-013-2668-7)
- [9] Y. Giomataris et al., Nucl. Instrum. Meth. A **376**, 29 (1996)
- [10] S. Andriamonje et al., J. Instrum. **5**, P02001 (2010)
- [11] N. Colonna et al., *A software compensation technique for fission measurements at spallation neutron sources*, Under preparation
- [12] A. Ferrari et al., Tech. Rep. CERN 2005-10, INFN/TC\_05/11, SLAC-R-773 (2005)
- [13] G. Battistoni et al., AIP Conf. Proc. **896**, 31 (2007)
- [14] M. Herman et al., Nucl. Data Sheets **108**, 2655 (2007)
- [15] R. Capote et al., Nucl. Data Sheets **110**, 3107–3214 (2009)